1990 SCA CONFERENCE PAPER NUMBER 9010

PSCAAR2x

PORE STRUCTURE CHARACTERISTICS OF LOW PERMEABILITY SHALES FROM DEEP FORMATIONS*

T.J. Katsube
Geological Survey of Canada
601 Booth St.Ottawa, Ontario, K1A 0E8

T.B. Murphy
Mineralogy Inc., 3228 E 15th st., Tulsa, Oklahoma, 74104, USA.
(Formerly at K&A Energy Consultants Inc.
6849 East 13th St., Tulsa, Oklahoma 74112 USA)

M.E. Best
Geological Survey of Canada
Atlantic Geoscience Centre
PO Box 1006, Dartmouth, Nova Scotia, B2Y 4A2

and

B.S. Mudford
UNOCAL Science and Technology Division,
376 South Vulencia Blvd., Brea, CA 92621 U.S.A.

May 25, 1990

CONTENTS

*: For submission to the 1990 SCA Annual Technical Conference.

PORE STRUCTURE CHARACTERISTICS OF LOW PERMEABILITY SHALES FROM DEEP FORMATIONS

T.J. Katsube
Geological Survey of Canada
601 Booth St.Ottawa, Ontario, K1A 0E8

T.B. Murphy
Mineralogy Inc., 3228 E 15th st., Tulsa, Oklahoma, 74104, USA.
(Formerly at K&A Energy Consultants Inc., Tulsa, Oklahoma)

M.E. Best
Geological Survey of Canada, Atlantic Geoscience Center,
PO Box 1006, Dartmouth, Nova Scotia, B2Y 4A2

B.S. Mudford
UNOCAL Science and Technology Division,
376 South Vulencia Blvd., Brea, CA 92621 U.S.A.

ABSTRACT

A petrophysical study consisting of porosity, permeability, formation factor and electrical resistivity measurements have been carried out on a set of shale samples taken at depths between 4500m and 5600m in the Venture Gas field offshore Nova Scotia. In addition, shale texture analysis, which includes scanning electron microscope analysis were performed on some of the samples. The purpose of the study is to obtain information on the mechanisms related to the porosity and permeability changes with progressive depths during sedimentary basin development. This information is necessary for quantitative sedimentary basin modelling, and to understand the reasons for the very low permeabilities exhibited by many tight shales.

A previous study indicated that the permeabilities of these shales are of the order of 10^{-22}-10^{-20} m^2 and that this is because the main flow paths are very tortuous with pore sizes in the order of 8 to 16nm, and with porosity concentrated in the extremely small pores.

Results of this study suggests the existence of a network of clay-lined surfaces that do not necessarily coincide with the network of pores. This implies that even when cementation occurs and completely blocks the pores to fluid flow, it does not necessarily prevent the transport of chemical species by diffusion, the network of clay-lined surfaces most likely being the pathway. Lack of clay-lined surfaces in well cemented rocks could not only isolate the pores, but could cause resistance to later development of pores by dissolution. Well-cemented shales with little or no clay-lined surfaces may play an important role in preserving porosity during basement development, and preserving high pressure fluids.

INTRODUCTION

Modelling studies (e.g. Burrus et al., 1988) indicate that shales play a dominant role in the development of fluid migration pathways during the evolution of sedimentary basins. Little is known about the petrophysical properties of shales, other than the fact that their permeability is extremely low, less than 10^{-21} m^2 for tight shales (Luffel and Guidry, 1989; Morrow et al., 1984; Mudford and Best, 1989). In particular, little is known about the pore structure and its relation to permeability. It is this property that controls fluid flow in shales. Although such data are readily available for sandstones, the lack of data for shales leads to significant uncertainty in the prediction of quantitative basin models, whose output currently relies on assumed or average shale properties. Therefore, the acquisition of petrophysical data for shales, especially tight shales at depth, is essential for further development of such models (e.g. Smith, 1971; Welte and Yukler, 1981; Ungerer et al., 1984; and Wei and Lerche, 1988).

A recent paper (Katsube, et al., in preparation) presents the results of a petrophysical study that analyzes the pore structure of 10 shale samples obtained from depths between 4700m and 5600m (Table 1) in three wells located in the Venture Gas Field, offshore Nova Scotia. It indicates that the extremely low permeabilities of these shales ($1.3x10^{-22}$-$1.6x10^{-20}$ m^2) occur because the fluid flow path consists of a network of very tortuous pores with small diameters, of the order of 8-16nm. However, the mechanisms relating the progressive decrease of permeability and porosity to compaction and diagenetic processes are poorly understood. The only data available relates permeability and porosity to stress, although even that is limited. This paper presents the results of investigating the use of several physical parameters to study the relationship between diagenetic processes and the petrophysical characteristics of these shales.

METHOD OF INVESTIGATION

Approach

Petrophysical study of the 10 shale samples from the Venture Gas Field consists of permeability, porosity, formation factor, mercury porosimetry, and stress-strain measurements. Results of these investigations have been partially reported in Katsube, at al., (in preparation). Permeability of two samples, using the transient decay method was measured as a function of pressure. Confining pressures of up to 70 MPa were applied (Figure 1). This paper concentrates on the results of mercury porosimetry analysis, effective porosity, formation factor and some new data consisting of electrical resistivity and shale texture analysis. The texture analysis includes X-ray diffraction analysis (XRD), scanning electron microscope (SEM) and petrographic thin section analysis (PTA).

Mineralogy and Sample Preparation

Cylindrical plugs with a diameter of 1 inch (2.54 cm) were cored in the vertical direction from 4 inch (10.16 cm) split core samples for the three Venture wells studied. Such plugs were obtained for all 10 samples. They were cut to a thickness of 1 cm for permeability measurements, and 0.5-1.0 cm for formation factor, porosity and mercury porosimetry measurements.

All 10 shale samples have slight variations in kaolinite, calcite and dolomite content according to XRD analysis. Quartz, mica and chlorite are major components in all 10 samples. Kaolinite is a major component in sample number 10, a minor component in 8 and 9, with only a trace in 5. Calcite is a major component in sample numbers 2, 6 and 9, and a minor component in 1 and 10. Dolomite is a minor component in sample numbers 9 and 10, with only a trace in 6.

Shale texture analysis consisting of XRD, SEM and PTA has been carried out on sample, numbers 4, 9 and 10, by K & A Energy

Consultants, Inc. (Tulsa, Oklahoma).

Porosity and Formation Factor

The effective porosity (Φ_E), which reflects the total pore volume excluding isolated pores, was determined by the immersion technique. The volume of pore space is determined from the difference in mass between oven-dried rock specimens and the same specimen saturated with distilled water. Further details of this technique are described in Katsube and Walsh (1987) and Katsube and Hume (in press).

In order to eliminate the erroneous effect of electrically conductive layers on the pore surfaces when determining the formation factor, measurements of bulk electrical resistivity are made on rock specimens saturated with solutions of different salinities (0.02, 0.05, 0.10, 0.20 and 0.5 M NaCl). The results are then inserted into the Patnode and Wyllie (1950) equation. Further details of this technique are described in Katsube and Walsh (1987), and Katsube and Hume (in press).

Mercury Porosimetry

The pore size distribution of porous materials is determined by mercury intrusion porosimetry. The mercury porosimeter used for these measurements is capable of generating pressures of 420 MPa which is high enough to force mercury into pores that are as small as 3.0 nm in diameter. Values of θ=30 and Y=0.48 N/m have been used in the Washburn equation (Rootare, 1970), with equilibration times of 10 and 30 seconds for low and high pressures, respectively. A good review of the technique is given in Rootare (1970). Further details of the methods used in these measurements are described in Katsube and Walsh (1987).

Electrical Resistivity Measurements

Both the bulk resistivity, ρ_R, and surface resistivity, ρ_C, of these shales were measured. The bulk resistivity is the resistivity

of the water saturated rock, which includes all effects such as the pore water resistivity, pore structure (represented by the formation factor) and the pore surface resistivity. The surface resistivity is the resistivity of the pore surfaces, and its value is derived from the Patnode and Wyllie equation (Patnode and Wyllie, 1950) when determining the formation factor. The methods used to determine these resistivities are described in Katsube and Hume (1989).

RESULTS AND ANALYSIS

Results of shale texture analysis based on three samples indicate that these shales can be classified as silty shales, sample numbers 4 and 10, and sandy shale, sample number 9. Sample numbers 4 and 10 are organic-rich silty shales which display inter-bedded laminae of siltstone and shale. The fabric of the sandstone lamina of sample number 9 is characterized by a densely packed detrital framework consisting of very fine sand-sized, sub-rounded and very well sorted grains. It appears that these shales have undergone the following six stages of diagenesis:

1. Deposition and burial, with ongoing compaction and grain rearrangement of the interlaminated shales, silts, and sands.
2. Sulphate-reducing bacteria digesting the abundant organic matter, caused precipitation of pyrite cement during deposition and shallow burial.
3. Pyrite cementation may have been followed by an early stage of calcite cementation in the inter-granular pore space of the sandstone laminae.
4. Chemically meta-stable silt and sand grains were then leached to yield secondary grain-moldic and intragranular dissolution porosity.
5. Subsequently, these secondary voids were partially to completely filled with calcite and/or siderite cement

and/or authigenic clay minerals.

6. Late diagenesis of these sediments included the partial replacement of calcite cement with dolomite, ferroan dolomite and/or ankerite cement.

The 3rd and 6th stages of diagenetic sequence are not applicable to sample number 4. However, there are some traces of siderite cementation present, indicating that stage 5 of diagenetic sequence is present. Sample number 9 appears to have been through all six stages of diagenesis, with the final stage blocking the interconnecting flow paths. This process may have isolated all of the macropores. Apparently, sample number 10 has undergone all six stages of diagenesis, with dolomite cement ultimately replacing calcite cement. It may have gone through another stage of leaching that caused the present macropores. This may have been related to the micropores in the detrital and authigenic clay matrix.

The effective porosity (Φ_E) and formation factor of all 10 samples are listed in Table 1. The range of porosity values, 0.8-9.3%, is at the low end of published shale porosities, in the range of 4-50% (Daly et al., 1966; Parkhomenko, 1967; Magara, 1971). This is related to our samples being from a greater depth, the deepest in Daly, et al., (1966) being 2400m. The range of formation factor values, 240 - 1600, is not unusual for sedimentary rocks (Parkhomenko, 1967), except the extremely large value of 17600 for sample number 6. The tortuosity factor(a) and cementation factor(m) of the modified Archie equation, $F=a\Phi^{-m}$ (Winsauer et al., 1952,) are 1.82, and 1.75, respectively. These values resemble those of low porosity rocks (Keller, 1982; p.245). The true tortuosity and pocket porosity of 3.3 and 0.7 are obtained by plotting effective porosity against the reciprocal of the formation factor (Figure 2), in accordance to the pocket porosity model (Katsube et al., 1985: Katsube and Hume, in press). The true tortuosity is unusually large and the pocket porosity unexpectedly small for a sedimentary rock, suggesting a very complex network of fluid flow paths, with

relatively few blind and pocket pores.

The results of the mercury porosimetry measurements for all 10 samples are presented in Table 2. The partial porosity, Φ_a, which is the porosity contributed by each pore size range (e.g. 2.5-4.0nm, 4.0-6.3nm, etc.), is listed in the column under each sample. The total porosity, Φ_T, listed near the bottom of the table, is the sum of partial porosities (Φ_a). Typical pore size distributions shown in Figure 3 depict a relatively simple uni-modal population concentrated in the 2.5-25nm range. The geometric means of the pore sizes are of the order of 8.7-16.2nm. These are extremely small values (Katsube and Walsh, 1987), and to our knowledge, some of the smallest ever reported for rocks. Two types of shales have been identified on the basis of pore size distribution. One, typified by Figure 3a (Type-A) has scarcely any pore throats above 100nm, the other typified by Figure 3b (Type-B) has a pore size distribution continuing above 1000nm. Samples number 2,6,7 and 9 fall in the Type-A category, number 1,3,5,8 and 10 in Type-B, and number 4 in-between (Type-AB).

The bulk electrical resistivity and surface resistivity for all 10 samples are listed in Table 1. The bulk resistivity values, 100-600 ohm-m, are about one order of magnitude larger than the electrical log resistivities (Mudford and Best, 1989) measured in the boreholes from which these samples were taken. This may be due to the high salinity of the water in the formations, a condition absent for laboratory measurements. The values for ρ_C/ρ_R, also listed in Table 1, represent the influence that pore surface resistivity has on the bulk resistivity of the sample. A value close to unity implies that the effect of the pore surface resistivity is dominant. On the other hand, a value considerably larger than unity implies that the surface effect is relatively small, and that the effect of the pore water is significant. Since this parameter can not be less than unity (Katsube and Hume, 1989), a value smaller than unity is interpreted as 1.0.

The average pore size, d, of the flow paths for fluids and ions calculated from permeability (k) and formation factor (F) values using the equation in Walsh and Brace(1984): $d=\sqrt{12Fk}$, for samples number 1 and 10 are 11.1 nm and 9.0 nm, respectively (Katsube et al., in preparation). These are comparable with the geometric means, of 10.0 nm and 13.1 nm, derived from the mercury porosimetry measurements (Table 2). This suggests that the larger pores, d > 25nm, are not part of the main flow paths, although they may be part of the inter-connected pore structure network. The results for all 10 samples for the pore size distribution, formation factor, effective porosity, total porosity and mineralogy are summarized in Figure 4 . The two porosities (effective determined by immersion, and total, by mercury porosimetry) show good agreement.

DISCUSSION

The shale samples have been divided into three types: Types A, B and AB, based on their poresize distributions (Katsube et al., in preparation). The samples can also be characterized by their values for porosity and electrical parameters (bulk resistivity, formation factor and resistivity ratios) listed in Table 1, as shown in Table 3.

Sample number 4, which lacks both significant carbonate cementation (diagenesis stages 3 and 6), shows intermediate (I-range) values for porosity, bulk resistivity and formation factor, a large (L-range) value for the resistivity ratio, ρ_C/ρ_R, and Type-AB poresize distribution. This suggests that there is a good interconnection between the macropores, with relatively small volumes of pore-lining clay. It is expected that the permeability of this sample will be at the larger end of values for these shales.

Sample number 9, which appears to have undergone all six

diagenetic processes, shows small (S-range) porosity, I-range of bulk resistivity, L-range of formation factor, S-range of resistivity ratio, and Type-A poresize distribution. This suggests that the cementation has almost completely blocked the connecting pores. The fact that the bulk resistivity and resistivity ratio are not high, implies that although the pores are extremely tight, there is some ionic connection, probably along clay layers lining the few macropores that are present, or along the grain surfaces, or both. This sample may also have a significant amount of isolated pore space due to the latest phase of carbonate cementation.

Sample No.10, appears to have undergone the six diagenetic processes plus a final dissolution process. It shows S-range bulk resistivity and resistivity ratio values, I-range effective porosity and formation factor values, and Type-B poresize distribution. This suggests it has a well developed interconnecting network for macropores and clay-lined surfaces. It is expected that Sample number 4 is more permeable, and Sample number 9 less permeable than Sample number 10 (1.6×10^{-20} and 1.3×10^{-22} m^2 at 2.5 and 70 MPa differential pressures, respectively).

Sample numbers 1, 3, 5, 8 and 10, which display Type-B poresize distribution all show similar characteristics for porosity and electrical parameters, that is I-S-I-S range characteristics for the four parameters (effective porosity, bulk resistivity, formation factor and resistivity ratios), except for sample number 8, which displays L and S-ranges for effective porosity and formation factor, respectively. This may suggest that these samples have textural characteristics similar to Sample number 10, with a good inter-connected network of both macropores and clay-lined surfaces, regardless of the many cementation processes they have undergone. Actually, the permeability of sample number 1 is similar to number 10, 8.5 and 0.7 nD at differential pressures of 2.5 and 40 MPa, respectively (Katsube, et al., in preparation).

Only sample number 4 falls within the Type-AB poresize distribution. Its porosity and electrical parameter characteristic of I-I-I-L are unique as well. Little consistency is seen in the porosity and electrical parameter characteristics for the 4 samples that fall in the Type-A poresize distribution. The closest are samples number 6 and 9, with one being S-I-L-L and the other S-I-L-S. This, most likely, implies that the two samples have a similar pore structure, except that the network of clay-lined surfaces which may exists to some extent in sample number 9 is completely absent in sample number 6. That is, the two samples probably were subject to the same diagenetic processes. However, the authigenic clay that may be coating the grains in sample number 9 are completely absent in sample number 6. Prediction of the diagenetic processes in samples number 2 and 7 is difficult at present, due to lack of data.

CONCLUSIONS

The results in this paper indicate that the addition of shale texture analysis and electrical resistivity data to the porosity, mercury porosimetry and permeability data considerably contributes to the understanding of the pore structure of these shales samples.

They also suggest the existence of a network of clay-lined surfaces that do not necessarily coincide with the network of macropores. This implies that even though the dolomite cementation that apparently takes place during one of the later diagenetic stages in these shales may completely block the pores to fluid flow, transport of chemical species by diffusion may still take place. The interconnecting network of clay-lined surfaces most likely would provide the pathway for diffusion. Lack of the clay-lined surfaces in a well cemented shale not only could cause complete isolation of pores, but could also resist later development of new pores by dissolution. These surfaces are insignificant when a well developed, interconnected macropore

network exists. A well cemented shale, with little or no clay-lined surfaces, may play an important role in preservation of porosity during basement development and in the preservation of high pressure fluids.

The combined use of effective porosity, bulk resistivity, surface resistivity and formation factor play an important role in detecting and estimating the significance of the clay-lined surfaces.

ACKNOWLEDGEMENTS

The authors are grateful to COGLA (Canada Oil and Gas Lands Administration), in Halifax Nova Scotia, for providing the core samples used in this study.

REFERENCES

Burrus, J., Doligez, B., Ungerer, P. and Kuhfuss, A., 1988. A 2D simulation of hydrocarbon generation and migration in the Northern Viking graben: The Am. Soc. of Petroleum Geologists Bulletin, in press.

Daly,R.A., Manger,E.G. and Clark,S.P.Jr.,1966. Density of rocks: Sec.4(p.23) in Handbook of Physical Constants. The Geol. Soc. of Am., Inc. Mem. 97, 19-26.

Katsube, T.J. and Walsh, J.B., 1987. Effective aperture for fluid flow in microcracks: International Journal of Rock Mechanics and Mining Sciences and Geomechanics Abstracts, 24, 175-183.

Katsube, T.J. and Hume, J.P., in press, Formation factor and porosity of crystalline rocks: Geophysics.

Katsube, T.J., Percival, J.B. and Hume, J.P., 1985. Characterization of the rock mass by pore structure parameters: Atomic Energy of Canada Limited Technical Record, TR-299, 375-413.

Katsube, T.J. and Hume, J.P.,1989, Electrical resistivity of rocks from Chalk River: In Workshop Proceedings on "Geophysical and Related Geoscientific Research at Chalk River, Ontario", Atomic Energy of Canada Limited Report AECL-9085, 105-114.

Katsube, T.J., Mudford, B.S., and Best, M.E., in prep., Petrophysical Studies of Shales from the Scotian Shelf: Submitted to Geophysics.

Keller, G.V.,1982. Electrical properties of rocks and minerals: in Handbook of Physical Properties of Rocks, Vol.I(ed. Carmichael, R.S.), CRC Press, Inc., Florida, 217-293.

Luffel, D.L. and Guidry, F.K., 1989. Reservoir rock properties of Devonian shale from core and log analysis: The Society of Core Analysts, Annual Technical Conference Preprints, Vol. I, Aug. 2-3, Paper 8910.

Magara, K., 1971. Permeability considerations in generation of abnormal pressures: Soc. of Petroleum Engineers J., 11, 236-242.

Morrow, C., Shi, L. and Byerlee, J., 1984. Permeability of fault gauge under confining pressure and shear stress: J. of Geophys. Res., 89, 3193-3200.

Mudford, B.S. and Best, M.E.,1989. The Venture Gas Field, offshore Nova Scotia, A case History of overpressuring in a region of low sedimentation rate: AAPG Bulletin, 73, 1383-1396.

Parkhomenko, E.I., 1967. Electrical Properties of Rocks: Plenum Press, New York.

Patnode, H.W. and Wyllie, M.R.J.,1950. The presence of conductive solids in reservoir rocks as a factor in electric log interpretation: Transactions of the American Institute of Mining, Metallurgical and Petroleum Engineers, 189, 47-52.

Rootare, H.M., 1970. A review of mercury porosimetry: Perspectives of powder metallurgy, 5, 225-253.

Smith, J., 1971. The dynamics of shale compaction and evolution of pore fluid pressures. Mathematical Geology, 3, 239-263.

Ungerer, P., Bessis, F., Chenet, P., Durand, B., Nogaret, E., Chiarelli, A., Oudin, J. and Perrin, J., 1984. Geological and geochemical models in oil exploration; principles and practical examples: In Demaison, G. and Murris, R.J. (Eds.), Petroleum Geochemistry and Basin Evaluation, AAPG Memoir 35, 53-77.

Walsh, J.B. and Brace, W.F.,1984. The effect of pressure on porosity and the transport properties of rocks. Journal of Geophysical Research, 89, 9425-9431.

Wei, Z. and Lerche, I., 1988. Quantitative dynamic geology of the Pinedale anticline, Wyoming, USA; an application of a two dimensional simulation model: Applied Geochemistry, 3, 423-440.

Welte, D. and Yukler, M., 1981. Petroleum origin and accumulation in basin evolution - a quantitative model. The Am. Ass. of Petroleum Geologists Bull., 65, 1387-1396.

Winsauer, W.O., Shearin, H.M., Masson, P.H. and Williams, M., 1952. Resistivity of brine-saturated sands in relation to pore-geometry: Bull. AAPG, 36, 253-277.

Table 1: Petrophysical measurements of Venture gas field shale samples, offshore Nova Scotia.

Sample Number	Depth (m)	Φ_E (%)	ρ_R (Ω-m)	F	ρ_C (Ω-m)	ρ_C/ρ_R
01	4693.4	3.78	146	541	144	0.98
02	4694.9	5.07	280	236	391	1.40
03	4916.4	4.64	180	268	164	0.91
04	4962.5	5.79	205	452	606	2.96
05	5122.4	3.73	305	1030	353	1.16
06	5131.5	0.80	580	17600	1660	2.86
07	5271.6	5.39	139	433	138	0.99
08	5273.5	9.24	127	241	129	1.02
09	5553.65	0.962	385	1630	470	1.22
10	5556.9	5.75	121	343	127	1.05

ρ_R = Bulk resistivity
Φ_E = Effective porosity
F = Formation factor
ρ_C = Surface resistivity

Table 2. Porosity distribution (partial porosity, Φ_a) for different pore sizes, d, obtained from Mercury porosimetry.

Sample Number	1	2	3	4	5	6	7	8	9	10
d (nm) \					Φ_a (%)					
2 - 4	0.86	0.57	0.76	1.43	0.66	0.33	1.03	1.16	0.43	0.82
4 - 6	1.14	0.64	1.15	1.43	0.63	0.27	1.06	1.54	0.35	1.23
6 -10	1.00	1.03	1.15	1.21	0.58	0.38	1.11	1.83	0.46	1.10
10-16	0.47	1.24	0.79	0.84	0.21	0.30	0.87	1.85	0.35	0.58
16-25	0.28	2.06	0.52	0.48	0.18	0.08	0.42	0.72	0.22	0.30
25-40	0.14	0.49	0.37	0.28	0.13	0.03	0.21	0.31	0.11	0.22
40-63	0.11	0.28	0.26	0.28	0.08	0.05	0.19	0.23	0.11	0.16
63-	0.08	0.18	0.13	0.22	0.08	0.03	0.08	0.13	0.05	0.08
100-	0.11	0.34	0.13	0.20	0.11	0.03	0.13	0.18	0.05	0.14
160-	0.06	0.21	0.05	0.11	0.05	0.00	0.05	0.08	0.00	0.08
250-	0.06	0.00	0.08	0.08	0.03	0.00	0.03	0.08	0.00	0.08
400-	0.06	0.00	0.03	0.11	0.11	0.00	0.00	0.08	0.00	0.05
630-	0.03	0.00	0.05	0.03	0.03	0.00	0.00	0.03	0.00	0.08
1000-	0.03	0.00	0.05	0.00	0.05	0.00	0.00	0.10	0.00	0.08
1585-	0.00	0.00	0.05	0.00	0.05	0.00	0.00	0.05	0.00	0.05
2512-	0.00	0.00	0.03	0.00	0.00	0.00	0.00	0.00	0.00	0.03
Φ_T	4.41	7.04	5.61	6.70	2.98	1.50	5.19	8.37	2.13	5.10
d^7	10.0	16.2	13.3	11.1	13.6	8.7	9.5	11.9	10.0	13.1
D	2.77	2.58	2.62	2.80	2.64	2.73	2.65	2.57	2.69	2.74

Φ_a = Partial porosity (%)
Φ_T = Total porosity (%)
d^7 = Mean(geometric) poresize (nm)
D = Density (g/cc)

Table 3. Definition of large, intermediate and small ranges for porosity, formation factor and electrical parameters.

Category	Units	Large (L)	Intermediate (I)	Small (S)
Effective Porosity (Φ_E)	%	> 6.0	2.0 - 6.0	< 2.0
Bulk Resistivity (ρ_R)	Ω-m	> 600	200 - 600	< 200
Formation Factor		> 1100	300 -1100	< 300
Resistivity Ratio (ρ_C/ρ_R)		> 2.0	1.3 -2.0	< 1.3

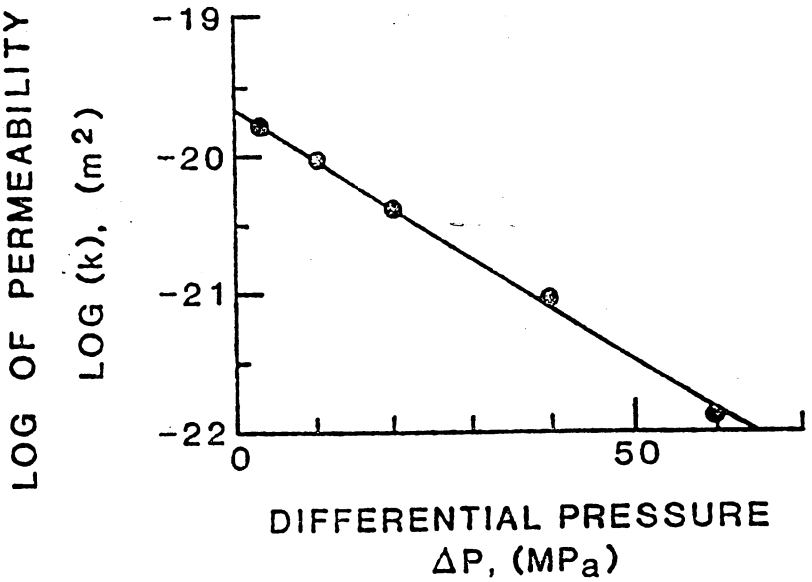

Figure 1: An example of permeability as a function of pressure for sample number 10 (from Katsube et al., in preparation).

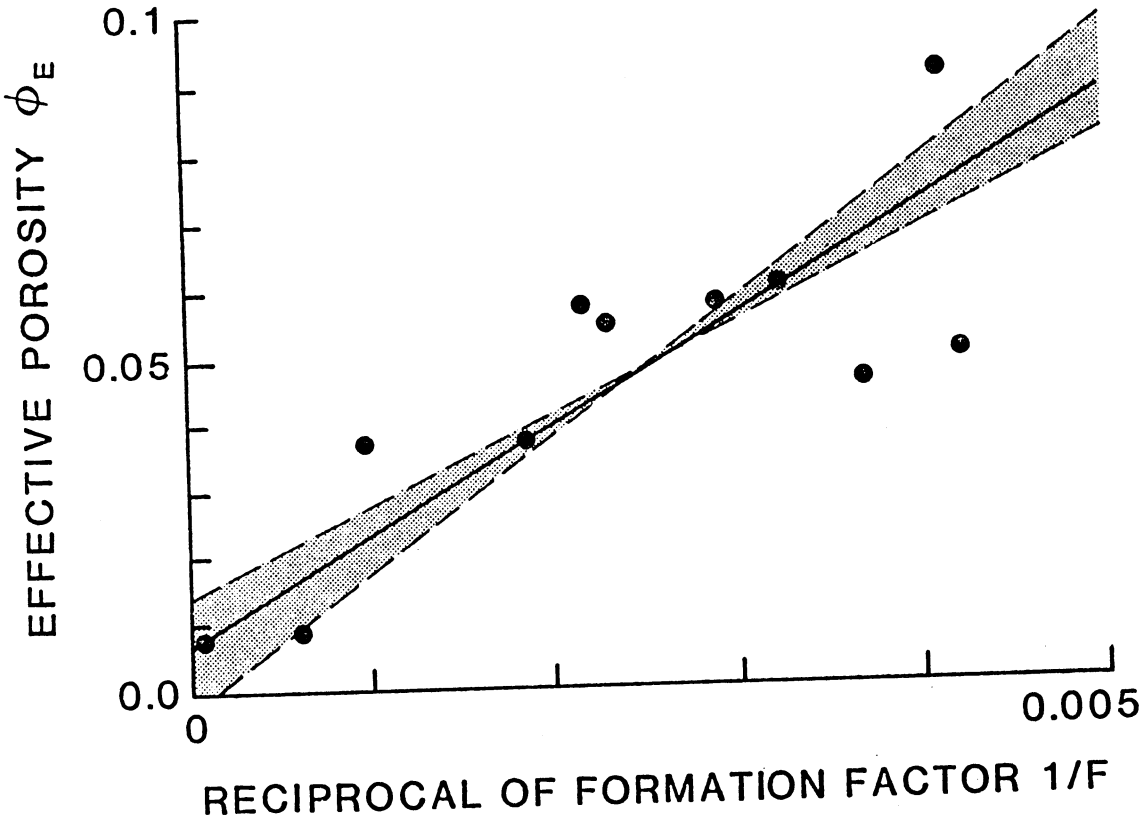

Figure 2: Effective porosity as a function of the reciprocal of formation factor for all 10 shale samples (from Katsube et al., in preparation).

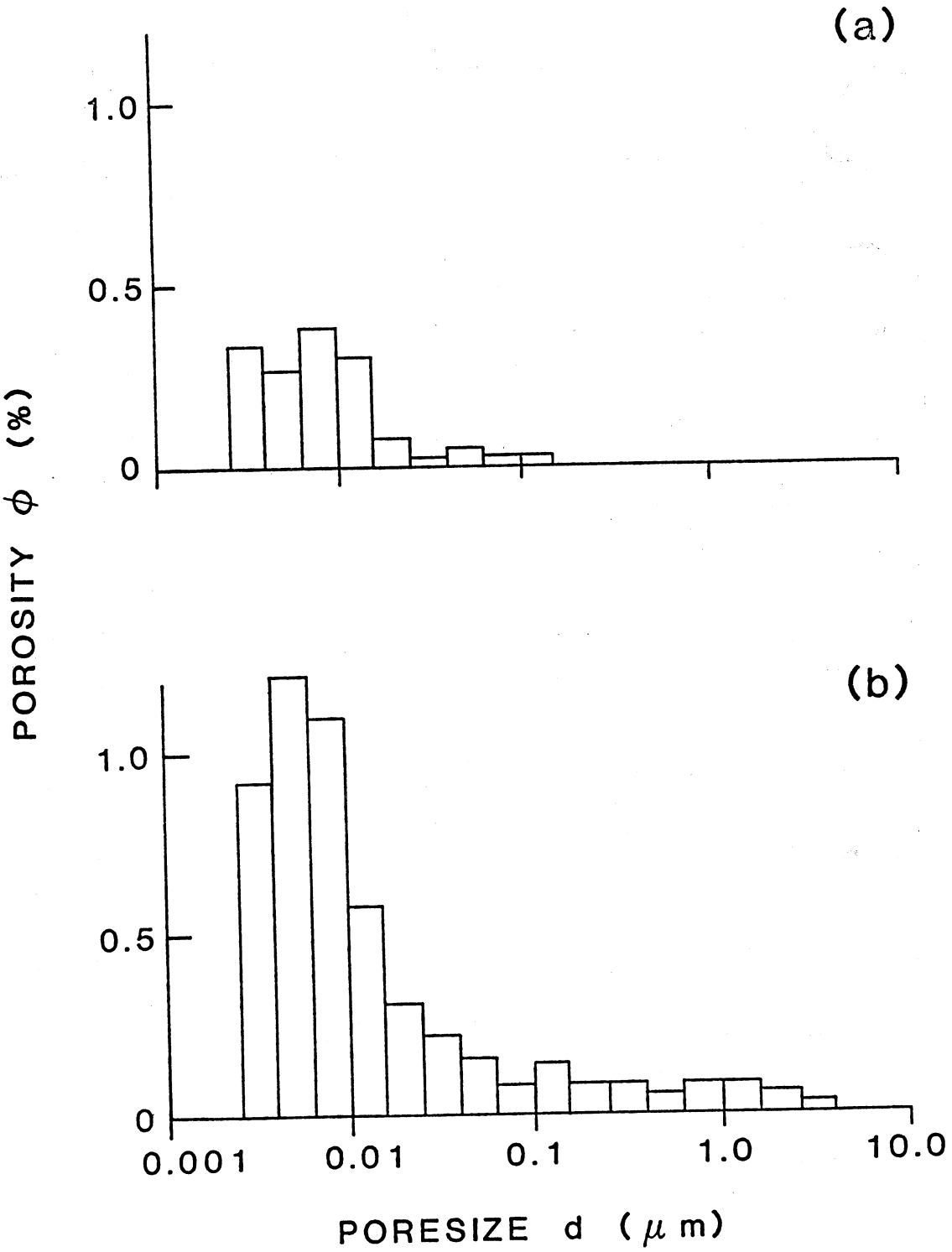

Figure 3: Typical pore size distribution (from Katsube et al., in preparation).

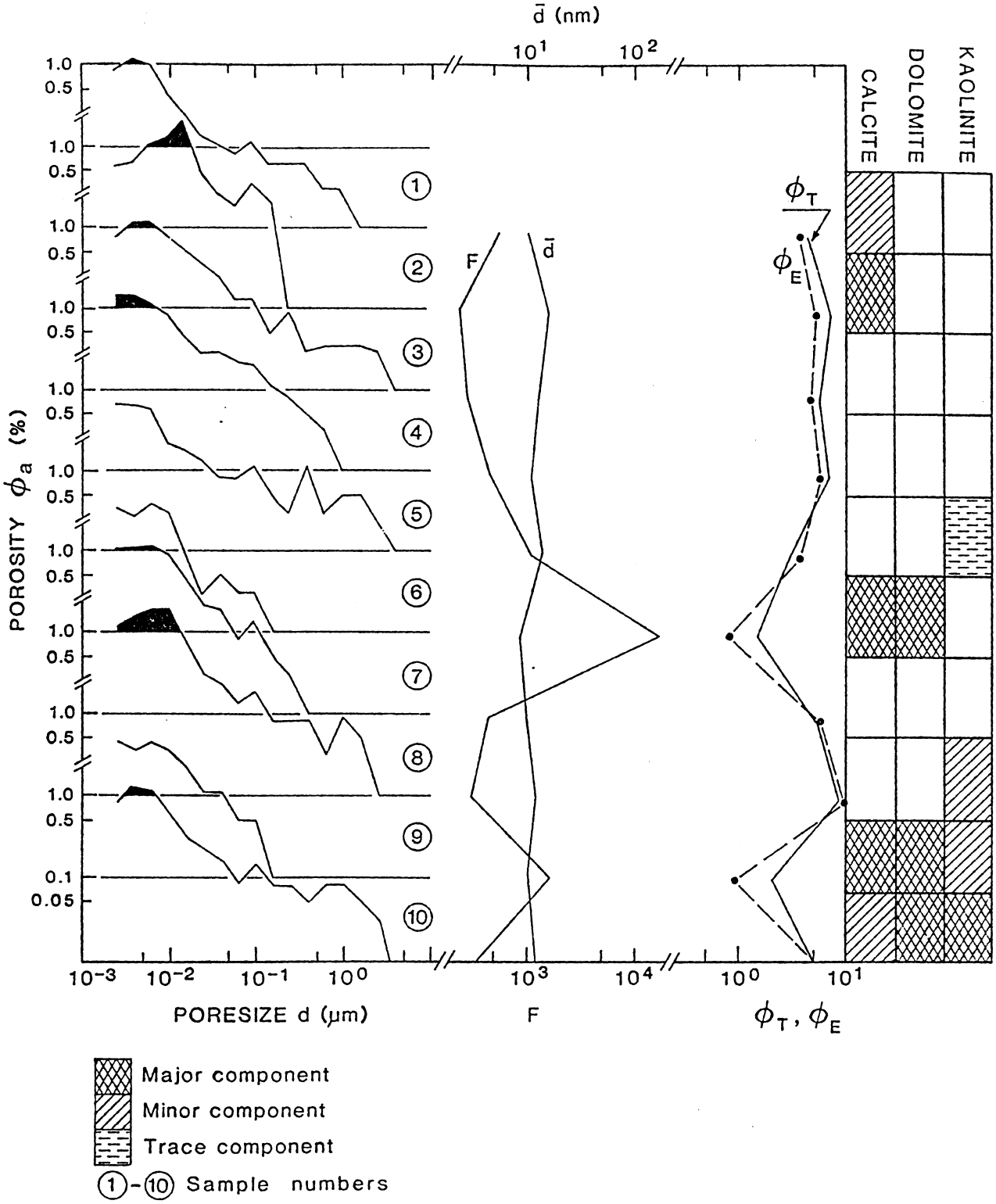

Figure 4: Results of pore size distribution, formation factor (F), effective porosity (Φ_E), total porosity (Φ_T) and mineralogy for the 10 samples.